Low Reynolds Number Aerodynamics of Leading Edge Flaps

A. R. Jones*, N. M. Bakhtian†, and H. Babinsky‡

Department of Engineering, University of Cambridge, Cambridge, CB2 1PZ, United Kingdom

Abstract

Recent efforts to develop MAVs have renewed interest in improving airfoil performance at low Reynolds numbers. Taking inspiration from birds, naturally maneuverable and efficient low Reynolds number fliers, the effects of a leading edge flap are investigated using a force balance and oil flow visualization. The avian leading edge flap is modeled using both a leading edge flap and a leading edge wire. It was found that the leading edge flap functions as a boundary layer trip rather than as a conventional high-lift device. Leading edge flap performance is compared to that of conventional surface-mounted transition trips over a range of Reynolds numbers from 4.0×10^4 to 1.2×10^5. It was found that while surface-mounted tape and wire trips are ineffective at high angles of attack, leading edge flaps and wires can greatly improve lift, even at the lowest Reynolds number. The leading edge devices were found to introduce disturbances to the flow which, at high angles of attack, propagate over the airfoil surface and prevent the formation of laminar separation bubbles.

Introduction

Recent efforts to develop micro air vehicles (MAVs) have renewed interest in low Reynolds number aerodynamics [1, 2, 3]. MAVs must be capable of executing precision maneuvers requiring high lift coefficients at low flight speeds and high angles of attack. Laminar separation bubbles, formed when a laminar boundary layer separates, transitions, and reattaches along the airfoil chord, are prevalent in this flight regime and can limit airfoil performance [4, 5, 6, 7]. To produce a functional MAV, high-lift devices capable of controlling laminar separation bubbles must be developed. The obvious sources of inspiration are the natural fliers capable of graceful and efficient flight – birds.

*PhD Research Student, Aerodynamics Laboratory, Department of Engineering, University of Cambridge, Trumpington Street, CB2 1PZ, UK, AIAA Student Member

†Research Student, Aerodynamics Laboratory, Department of Engineering, University of Cambridge, Trumpington Street, CB2 1PZ, UK, AIAA Student Member

‡Reader in Aerodynamics, Department of Engineering, University of Cambridge, Trumpington Street, CB2 1PZ, UK, AIAA Senior Member

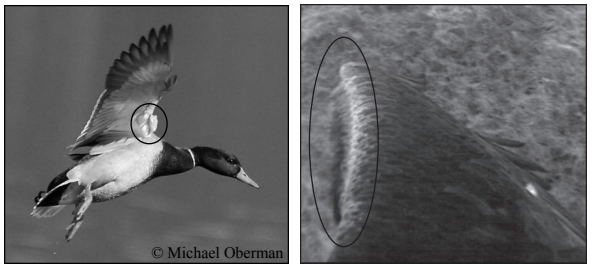

(a) Mallard landing

(b) Golden Eagle cruising (©BBC, 2004)

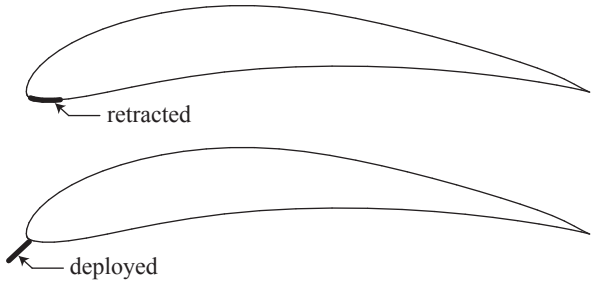

(c) Leading edge flap retracted and deployed

Figure 1: Leading edge flap as observed on bird wings on the approach to landing and during cruise.

A protruding flap of feathers as shown in Figure 1 has been observed at the leading edge of bird wings. This leading edge flap deploys both during landing maneuvers when the wing is rapidly pitching up near deep stall and during cruising flight when the wing is at a more modest angle of attack. Carruthers et al. suggest that the leading edge flap deploys during landing to alleviate a pitch-up instability that arises on M-shaped wing planforms [8]. Others suggest that leading edge devices can eliminate laminar separation bubbles during cruising flight [9, 10].

The objectives of the current study are to ascertain the function of the avian leading edge flap in cruising flight, offer an explanation of the aerodynamic mechanisms which result in high lift, and to evaluate the benefits of the leading edge flap as a high lift device for MAVs. Experiments are performed at Reynolds numbers of 4.0×10^4, 7.0×10^4, 9.5×10^4, and 1.2×10^5 to represent the flight regime of large birds and MAVs. Because turbulators are the most common way to produce high lift at low Reynolds numbers, the effects of leading edge flaps on a low Reynolds number airfoil are compared to those of several conventional trips. Lift and drag forces are recorded and surface oil flow visualization performed for multiple turbulator types and designs.

Experimental Setup

Apparatus and methods

The experiments described here were performed in the University of Cambridge Engineering Department 1B low speed wind tunnel. The 1B is an open-return tunnel capable of speeds up to 25 ms^{-1} with a 0.715 m by 0.510 m working section. Turbulence intensity was measured using a hot-wire anemometry system and was found to be approximately 0.10% between 10 and 20 ms^{-1}.

An Eppler E423 airfoil with a chord length of 9.73 cm and a span of 71.0 cm, nearly the width of the tunnel, was used for all of the experiments described here. The airfoil was sting-mounted on an external Flow Dynamics Ltd 50 N Lift-Drag strain gauge balance. Lift, drag, and power input to the balance were recorded at 100 Hz by a Microlink 3000 data acquisition system. Lift and drag values were time averaged over 1 s. Force measurements were supplemented by surface oil flow visualization, performed using a mixture of kerosene, titanium dioxide, and oleic acid. Wind tunnel speed was measured using a pitot-static tube positioned upstream of the model and connected to a methylated spirits manometer. Each airfoil configuration was tested at chord Reynolds numbers of 4.0×10^4, 7.0×10^4, 9.5×10^4, and 1.2×10^5 for $0^\circ \leq \alpha \leq 30^\circ$ in 1° increments.

Uncertainty and corrections

The primary source of uncertainty for the clean wing is the angle of attack setting, accurate to within 0.4°. The overall error in force coefficient measurements was found to be 3% accounting for errors in flow speed, angle of attack, bias error introduced during calibration, and sampling precision. Errors associated with the installation of leading edge flaps or wires are 4% for length, 5% for placement, and 4% for deployment angle. Due to these variations, the force coefficients for these configurations have an uncertainty closer to 8%. In the work presented here, we are primarily interested in the shapes of the lift-to-drag polar curves rather then the numerical values.

Wind tunnel boundary conditions were calculated using the methods of Pope and Harper [11]. Calculations of the solid two-dimensional blockage factor, wake blockage, and correction for streamline curvature lead to an effective C_l ranging from 0.92 to 0.98 and an effective C_d ranging from 0.93 to 0.99 of the uncorrected values. Corrections are small and thus are not applied to the data presented here. Error bars are omitted from the following plots for clarity.

Turbulators

The avian leading edge flap was modeled by the two devices shown in Figure 2: a leading edge flap and a leading edge wire. A 1.1 mm diameter full-span wire was mounted 5 mm ahead of the leading edge of the airfoil on 5 brackets. To form the leading edge flap, the gap between the wire and the airfoil was covered with tape to form an airtight flap. The flap position on the leading edge of the airfoil was defined by a placement angle θ and deflection γ with respect to the chord line as shown in Figure 3. To determine these angles, a photograph was taken of the airfoil with the leading edge device installed and the angles were measured using digital imaging software. For all leading edge flap and wire tests the flap placement angle θ was 57°. Both devices were tested for flap deflection angles γ of 11°, 43°, and 75°. For the airfoil configurations with a leading edge flap, force coefficients were calculated using an adjusted chord value accounting for the flap chord. Angles of attack, however, were defined with respect to the clean airfoil chord line regardless of airfoil configuration.

Full-span tape turbulators of width 19 mm and thickness 0.12 mm or 0.24 mm were installed on the airfoil at both 2% and 5% chord as shown in Figure 3. The chordwise location of the tape turbulators was defined from the leading edge of the airfoil to the upstream edge of the tape. Similarly, full-span surface wire turbulators were installed at the same location by epoxying 1.1 mm diameter wire to the airfoil.

Results and Discussion

Clean airfoil

For the range of Reynolds numbers tested here, the laminar separation bubble is the dominant flow feature and the development of this bubble has a huge impact on airfoil performance. At relatively high Reynolds numbers, the separated laminar boundary layer transitions and eventually reattaches downstream, forming a separation bubble as sketched in Figure 4(a). At lower Reynolds numbers, there is insufficient room on the airfoil chord for the boundary layer to transition and reattach. The flow remains separated with a large region of recirculating flow at the trailing edge as in Figure 4(b). This type of flow is unsteady and the separation point can move along the chord.

Drag polars for a clean E423 airfoil at Reynolds numbers of 4.0×10^4, 7.0×10^4, 9.5×10^4, 1.2×10^5, and 1.4×10^5 are given in Figure 5. The airfoil performs well at $Re = 1.4 \times 10^5$, reaching a maximum C_l value over 2.0 despite the

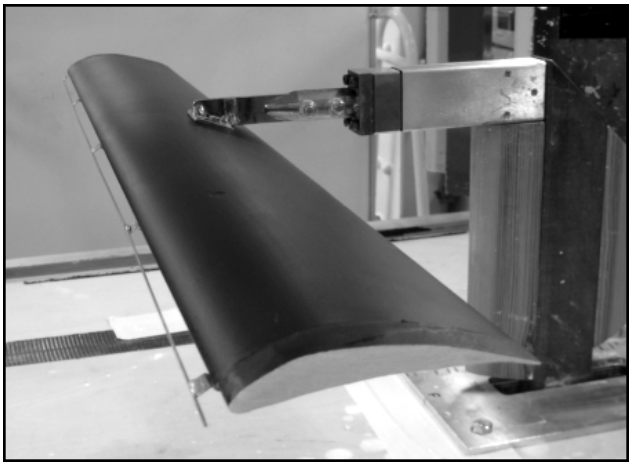

(a) Wire

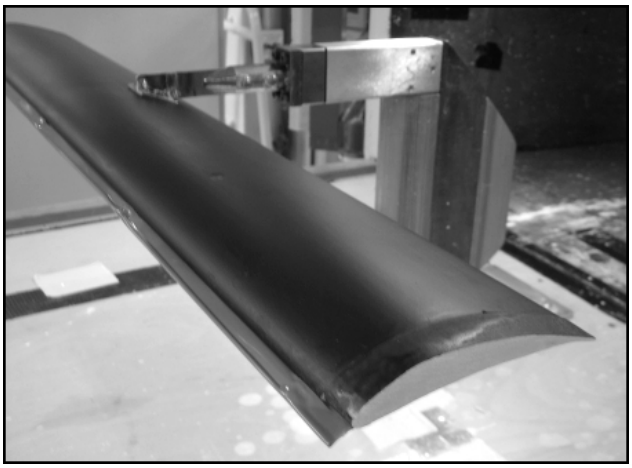

(b) Flap

Figure 2: Leading edge device installation.

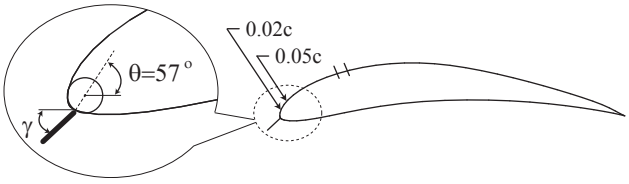

Figure 3: Turbulator placement. Leading edge devices are defined by angles θ and γ with respect to the chord line. Tape trips begin at 2% and 5% chord and extend to the marks downstream.

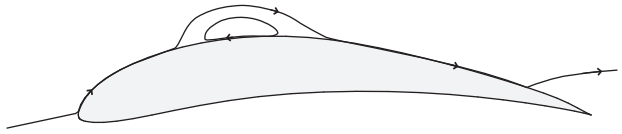

(a) Laminar separation bubble with subsequent trailing edge separation.

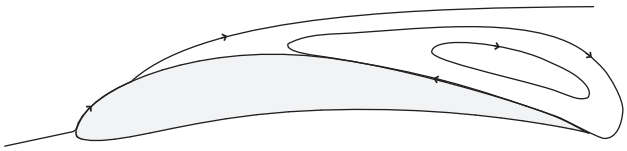

(b) Separated flow without reattachment.

Figure 4: Sketch of streamlines over an airfoil with laminar boundary layer separation.

presence of a laminar separation bubble revealed by the oil flow visualization in Figure 6. As the Reynolds number decreases, performance deteriorates. At $Re = 1.2 \times 10^5$ the laminar separation bubble has a much greater effect on the flow over the upper surface. As the angle of attack increases to 8°, the separation bubble grows and bursts resulting in low lift. At $\alpha = 12°$ the separation bubble has moved upstream allowing the boundary layer to reattach, improving lift. As the angle of attack increases further, the separation bubble continues to grow, burst, and reattach, causing C_l values to vary with the current state of the bubble. Below $Re = 1.2 \times 10^5$ the laminar boundary layer separates soon after the leading edge and is unable to reattach. Flow over the airfoil is largely separated, even at low angles of attack. As the angle of attack increases, the separation point moves upstream, but reattachment does not take place and lift remains low, leveling off near $C_l = 1.5$.

Surface-mounted trips

As seen in Figures 7 and 8, both the tape and wire surface-mounted trips were found to improve lift for low to mid angles of attack, but both were ineffective at high angles of attack. Drag polars for these turbulators are characterized by a smooth rise in C_l with angle of attack before smoothly dropping down to clean wing values. All trip designs were found to improve lift except at the lowest Reynolds numbers. Thin tape trips produced the highest lift. All of the tape trips were ineffective at $Re = 4.0 \times 10^4$. Chordwire position was not critical for the tape or wire, especially at higher Reynolds numbers. The surface-mounted wire trip was not as effective as the tape trip, likely due to the

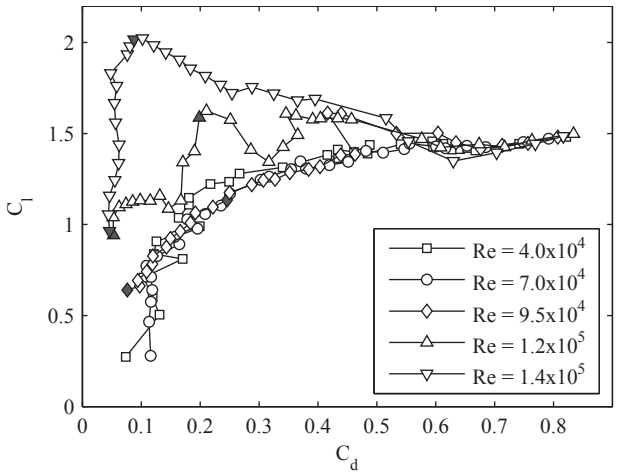

Figure 5: Lift-to-drag polars for a clean E423 airfoil. Shaded data points are $\alpha = 0°$, $12°$ corresponding to oil flow visualization.

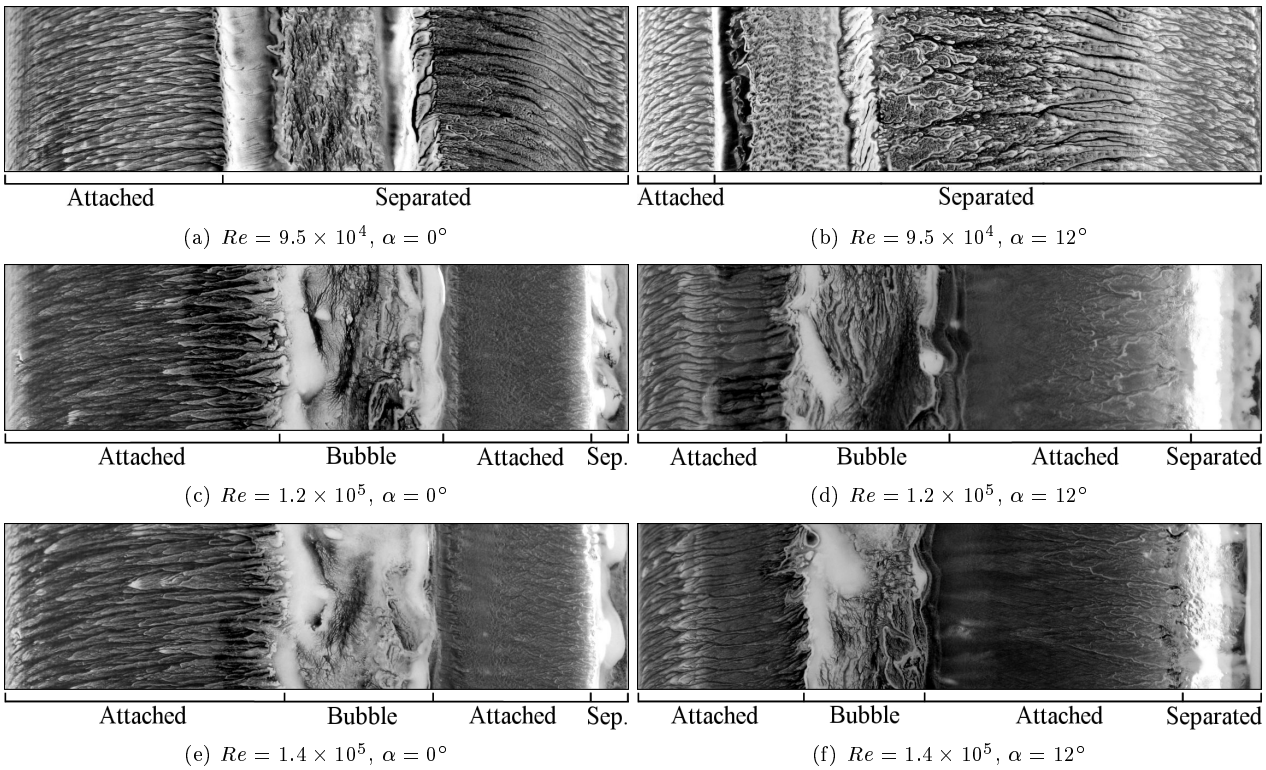

(a) $Re = 9.5 \times 10^4$, $\alpha = 0°$ (b) $Re = 9.5 \times 10^4$, $\alpha = 12°$

(c) $Re = 1.2 \times 10^5$, $\alpha = 0°$ (d) $Re = 1.2 \times 10^5$, $\alpha = 12°$

(e) $Re = 1.4 \times 10^5$, $\alpha = 0°$ (f) $Re = 1.4 \times 10^5$, $\alpha = 12°$

Figure 6: Surface oil flow on the upper surface of a clean E423 airfoil. Flow is from left to right.

Table 1: Leading edge flap and wire critical angles of attack.

Reynolds number	LE Device	α_{cr}
7.0×10^4	11° flap	9°
	43° flap	13°
	75° flap	26°
	11° wire	7°
	43° wire	11°
	75° wire	20°
9.5×10^4	11° flap	6°
	43° flap	10°
	75° flap	27°
	11° wire	5°
	43° wire	11°
	75° wire	19°

large trip height, but was the only surface-mounted trip effective at $Re = 4.0 \times 10^4$. Oil flow visualizations in Figure 11 reveal that the 0.12 mm tape trip at 2% chord increases the attached flow over the airfoil but fails to trip the boundary layer and prevent the formation of a laminar separation bubble.

Leading edge devices

Drag polars for the leading edge flap and wire are given in Figures 9 and 10. These plots are characterized by a sharp increase in C_l at a critical angle of attack α_{cr}. Below α_{cr}, lift is lower and drag is higher than that of the clean airfoil, but once this angle of attack has been reached airfoil performance improves dramatically and the high C_l values are relatively constant for all higher α. For both leading edge devices it was found that steeper deflection angles, larger γ, delayed their effectiveness to higher angles of attack. This effect is most obvious in Figure 10(b) and has been summarized in Table 1.

At $Re = 4.0 \times 10^4$ only the shallowest flaps, $\gamma = 11°$ and 43°, produce an obvious lift improvement. For these two configurations a maximum C_l of 1.9 was achieved, very near that of the higher Reynolds numbers. At $Re = 7.0 \times 10^4$, the maximum lift coefficients for the $\gamma = 11°$ and 43° are 1.7 and 2.0, respectively. At $Re = 9.5 \times 10^4$, the $\gamma = 11°$ and 43° cases produce maximum lift coefficients of 1.6 and 1.8. At $Re = 1.2 \times 10^5$, the maximum lift coefficient is 2.0 with the $\gamma = 75°$ flap. The shallower flaps perform only slightly worse than they did at $Re = 9.5 \times 10^4$, but since clean

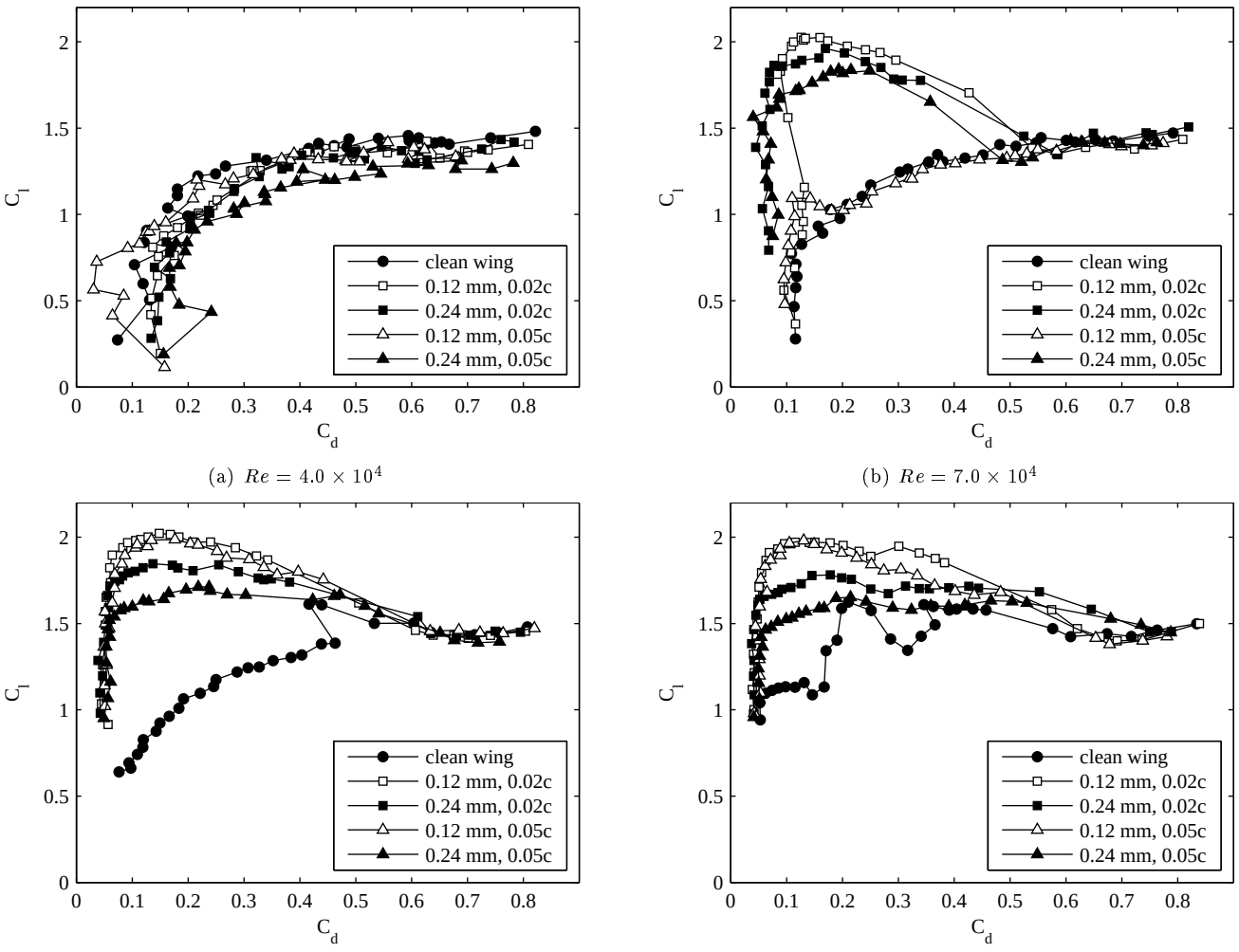

(a) $Re = 4.0 \times 10^4$

(b) $Re = 7.0 \times 10^4$

(c) $Re = 9.5 \times 10^4$

(d) $Re = 1.2 \times 10^5$

Figure 7: Drag polars for airfoil with surface-mounted tape trip.

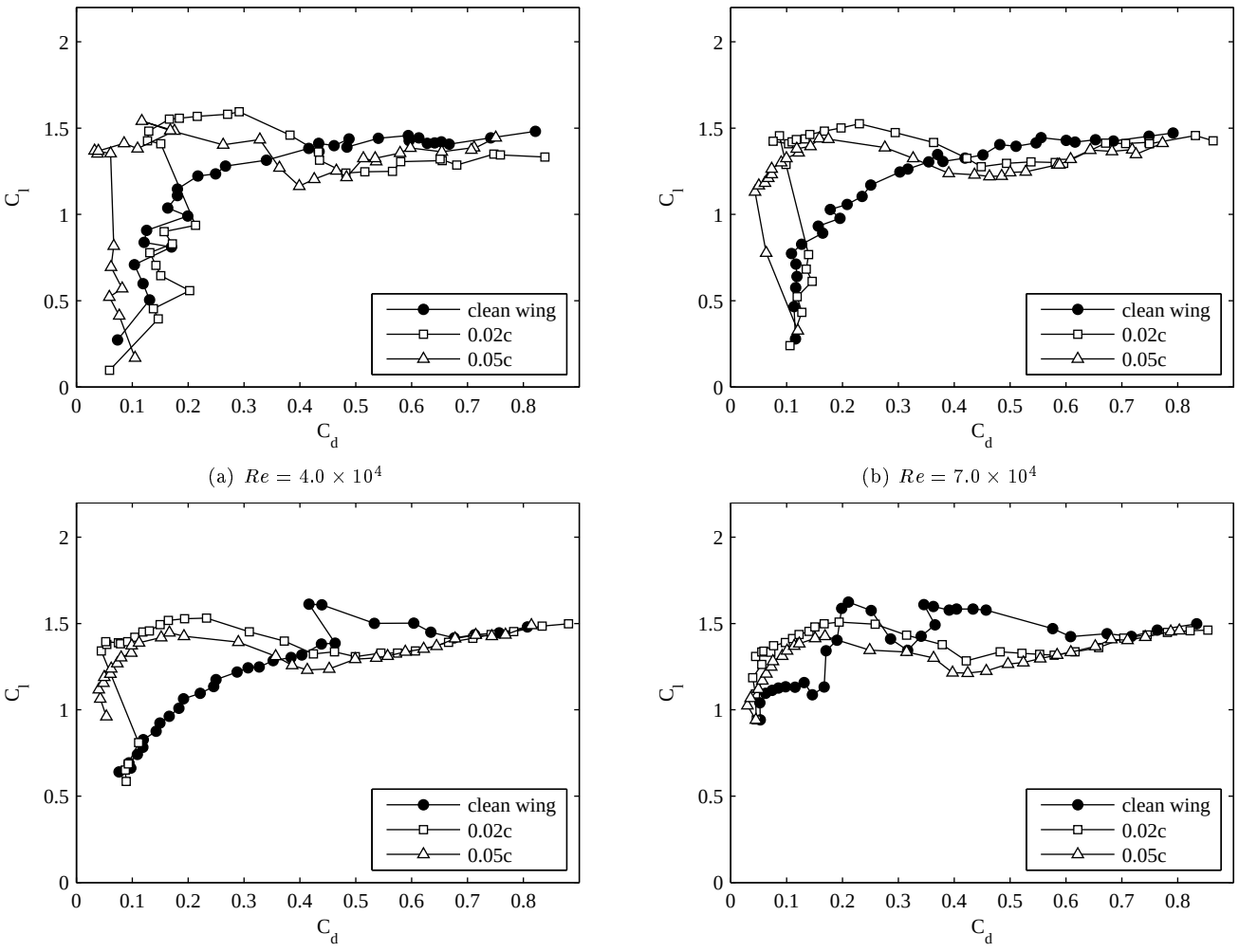

(a) $Re = 4.0 \times 10^4$

(b) $Re = 7.0 \times 10^4$

(c) $Re = 9.5 \times 10^4$

(d) $Re = 1.2 \times 10^5$

Figure 8: Drag polars for airfoil with surface-mounted wire trip.

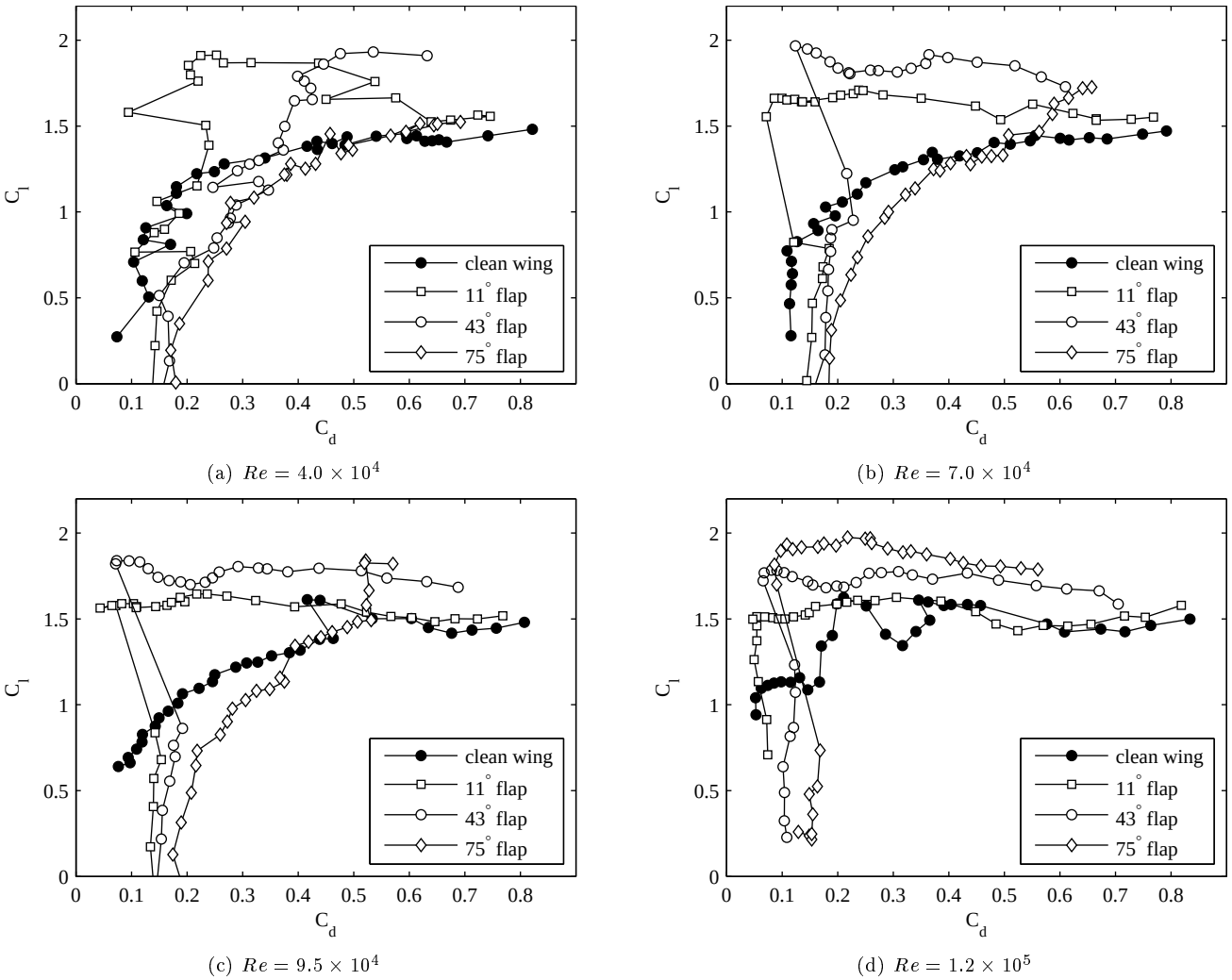

(a) $Re = 4.0 \times 10^4$

(b) $Re = 7.0 \times 10^4$

(c) $Re = 9.5 \times 10^4$

(d) $Re = 1.2 \times 10^5$

Figure 9: Drag polars for airfoil with leading edge flap. (Some data points at the lowest angles of attack are not shown.)

wing performance is better at the higher Reynolds number, these devices do not provide much of an improvement. At the highest angle of attack, $\alpha = 30°$, steeper flaps tend to have higher lift and lower drag.

Drag polars with the leading edge wire installed, given in Figure 10, are very similar to those with the leading edge flap. Again high lift at high angles of attack can be achieved even at the lowest Reynolds number. Like the flap, the wire inhibits airfoil performance at low angles of attack, but to a lesser degree. The maximum lift for the leading edge wire is slightly lower than the flap, 1.9 for $\gamma = 11°$ at $Re = 7.0 \times 10^4$, 9.5×10^4, and 1.2×10^5, occurring at $\alpha = 17°$, $20°$, and $17°$ respectively.

The oil flow visualization in Figure 11 shows that the leading edge flaps and wires prevent the formation of laminar separation bubbles. As evidenced by both the different shapes of the drag polar curves (Fig. 13) and surface oil flow visualizations (Fig. 11), the leading edge flap and wire produce high lift in a fundamentally different way than does the tape trip. Unlike the tape trip, these leading edge devices are ineffective at low angles of attack but produce a large increase in C_l at high angles of attack. This sudden change in flow behavior is thought to be a result of the device's position relative to the leading edge of the airfoil. As seen in Figure 12, the vortex shedding behind a leading edge wire would pass under the airfoil at low angles of attack. At a certain angle of attack, however, the flow disturbances would begin to pass over the upper surface of the airfoil, altering the development of the boundary layer. The effect of the leading edge flap is similar, with disturbances generated at the sharp leading edge. Slightly higher values of C_l near the critical angle of attack may be due to the filled in flap guiding more disturbed flow over the airfoil rather than losing the excited flow to the lower surface.

Conclusions

Observations of birds in flight have lead to the discovery of a flap of feathers which deploys at the leading edge of the wing during slow cruising flight and rapid pitch-up maneuvers such as approach to landing. In the current work a steady-flow case has been developed to compare the effects of a leading edge flap to those of other transition trips at low Reynolds numbers. This series of experiments has shown that the leading edge flap works as a transition trip, introducing disturbances into the flow which, at high angles of attack, propagate over the upper surface of the wing preventing the formation of a laminar separation bubble. Due to the geometry and placement of such a flap, it becomes effective only at high angles of attack, the same flight regime in which the avian flap has been observed.

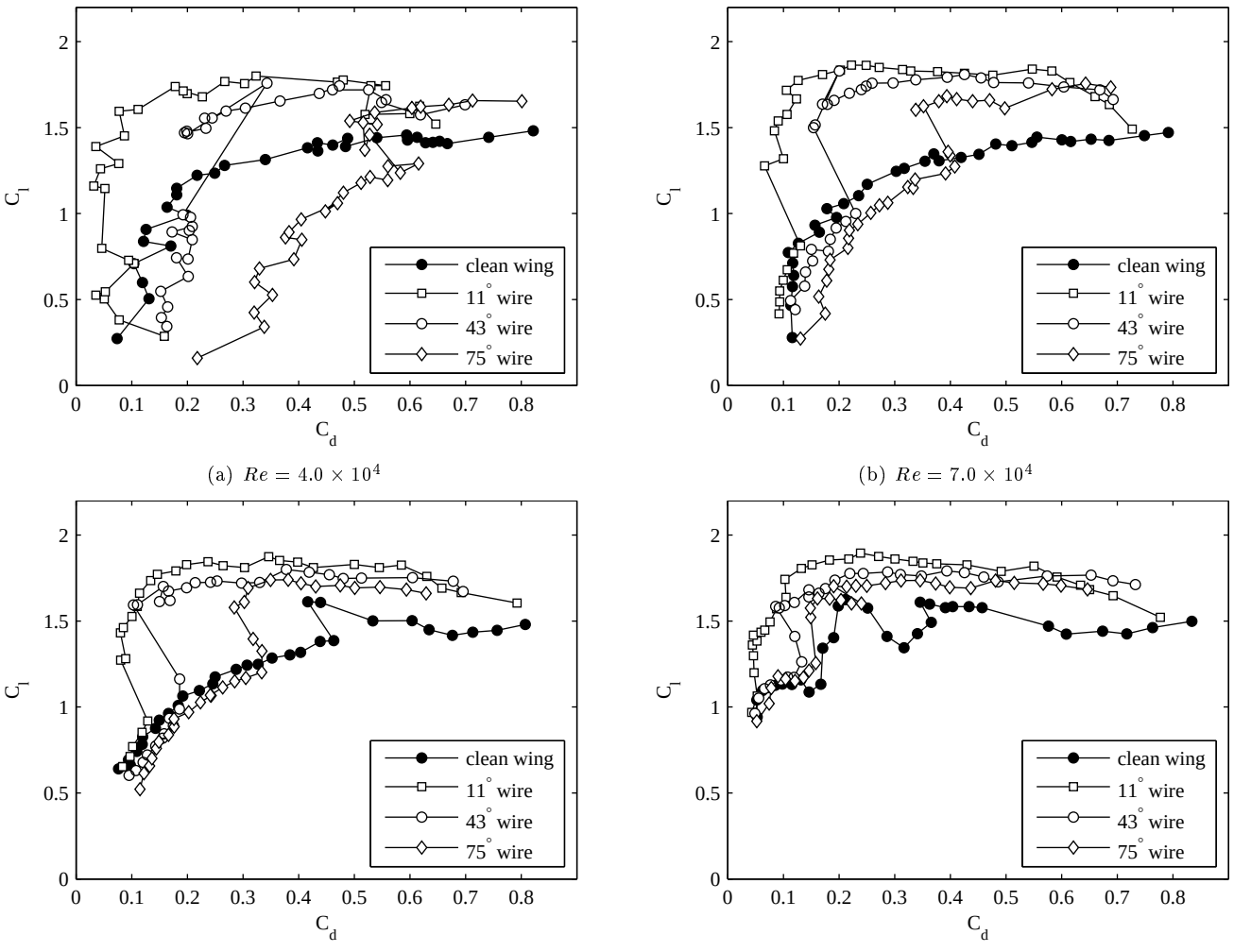

(a) $Re = 4.0 \times 10^4$

(b) $Re = 7.0 \times 10^4$

(c) $Re = 9.5 \times 10^4$

(d) $Re = 1.2 \times 10^5$

Figure 10: Drag polars for airfoil with leading edge wire.

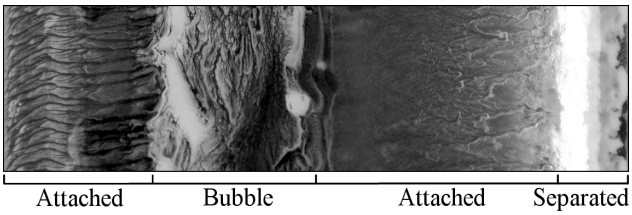

(a) Clean wing

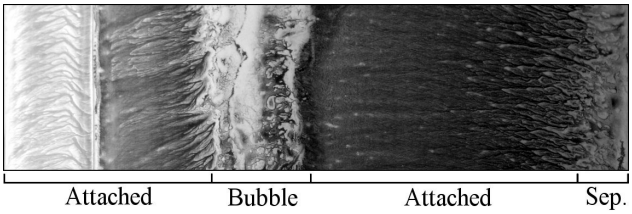

(b) Tape trip

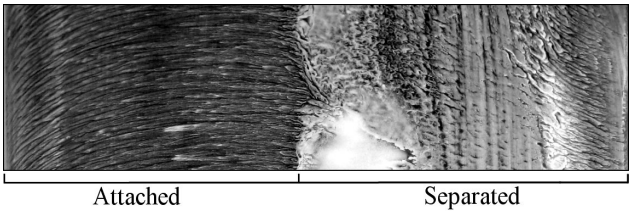

(c) Leading edge wire

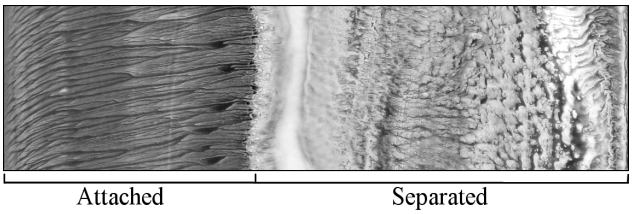

(d) Leading edge flap

Figure 11: Surface oil flow visualization for $Re = 1.2 \times 10^5$, $\alpha = 12°$. Flow is from left to right.

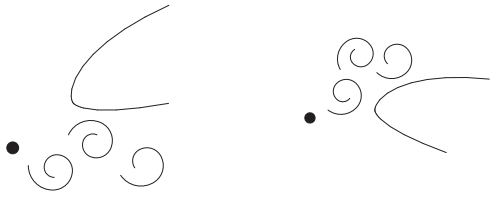

(a) Low α (b) High α

Figure 12: Effect of wire trip at low and high angles of attack.

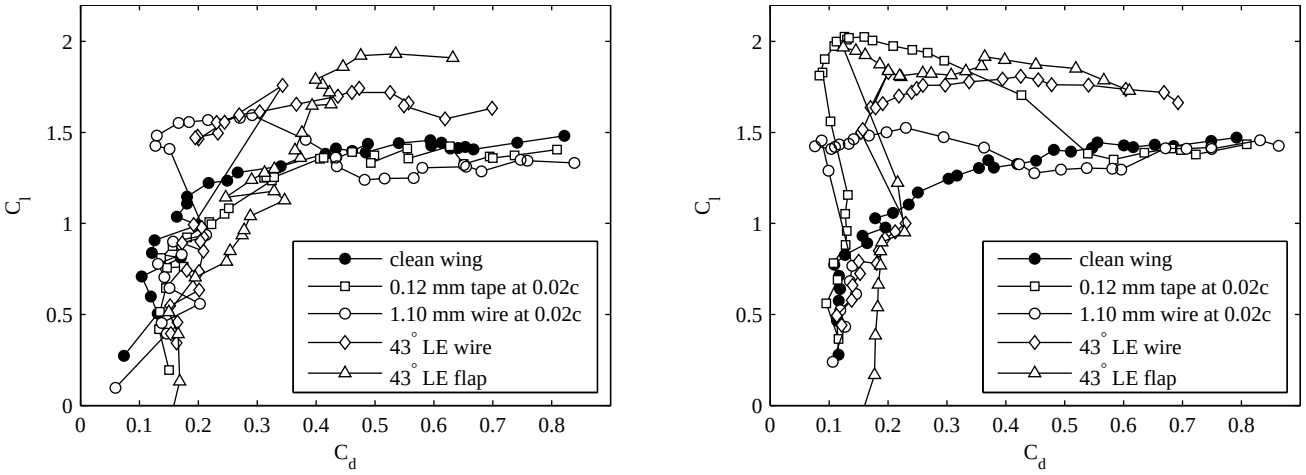

(a) $Re = 4.0 \times 10^4$

(b) $Re = 7.0 \times 10^4$

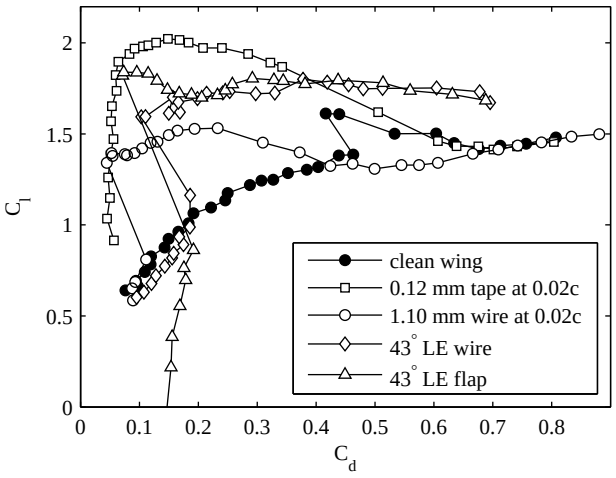

(c) $Re = 9.5 \times 10^4$

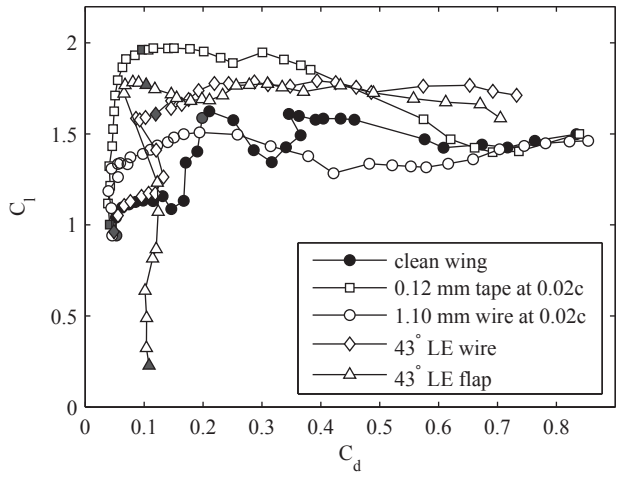

(d) $Re = 1.2 \times 10^5$

Figure 13: Drag polars for airfoil with surface-mounted tape trip, surface-mounted wire trip, leading edge flap, or leading edge wire. Shaded data points in (d) are $\alpha = 0°$, $12°$.

A study of flap design parameters has shown that shallower flap deflection angles become effective at lower angles of attack. Leading edge flaps were found to be effective high-lift devices at Reynolds numbers as low as 4.0×10^4. Conversely, more conventional tape trips are not effective at such low Reynolds numbers though effective tape trips were developed for Reynolds numbers as low as 7.0×10^4. These tape trips, however, are completely ineffective at high angles of attack, the flight regime of interest.

These results suggest that a leading edge flap can be used as a high lift device for low Reynolds number flight vehicles. The dynamic case of an automatically deploying flap as is seen on bird wings is of particular interest as such a device would not share the drag penalty at low angles of attack that is seen for the fixed flaps. Future work will focus on the development of an unsteady pitch-up test case and the design of an automatically deploying leading edge flap.

Acknowledgements

The authors gratefully acknowledge the funding provided by the Air Force Research Laboratory, the National Science Foundation, and the Winston Churchill Foundation.

References

[1] Mueller, T. J. and DeLaurier, J. D., "An Overview of Micro Air Vehicle Aerodynamics," *Fixed and Flapping Wing Aerodynamics for Micro Air Vehicle Applications*, edited by T. J. Mueller, Vol. 195 of *Progress in Astronautics and Aeronautics*, AIAA, Reston, VA, 2001, pp. 191–213.

[2] Mueller, T. J. and DeLaurier, J. D., "Aerodynamics of Small Vehicles," *Annual Review of Fluid Mechanics*, Vol. 35, January 2003, pp. 89–111.

[3] Pines, D. J. and Bohorquez, F., "Challenges Facing Future Micro-Air-Vehicle Development," *Journal of Aircraft*, Vol. 43, No. 2, 2006, pp. 290–305.

[4] Carmichael, B. H., "Low Reynolds Number Airfoil Survey, Volume I," NASA-CR-165803-Vol-1, November 1981.

[5] Gad-el Hak, M., "Control of Low-Speed Airfoil Aerodynamics," *AIAA Journal*, Vol. 28, No. 9, September 1990, pp. 1537–1552.

[6] Lissaman, P. B. S., "Low-Reynolds-Number Airfoils," *Annual Review of Fluid Mechanics*, Vol. 15, January 1983, pp. 223–239.

[7] Tani, I., "Low-Speed Flows Involving Bubble Separations," *Progress In Aeronautical Sciences*, Vol. 5, 1964, pp. 70–103.

[8] Carruthers, A. C., Taylor, G. K., Walker, S. M., and Thomas, A. L. R., "Use and Function of a Leading Edge Flap on the Wings of Eagles," AIAA Paper 2007-43, January 2007.

[9] Azuma, A., *The Biokinetics of Flying and Swimming*, Springer-Verlag, Tokyo, Ch. 3, 1992.

[10] Hertel, H., *Structure - Form - Movement*, Reinhold Publishing Corporation, New York, 1963.

[11] Pope, A. and Harper, J. J., *Low-Speed Wind Tunnel Testing*, John Wiley & Sons, Inc., New York, 1966.